

# Fluorogenic Tagging Methodology Applied to Characterize Oxidized Tyrosine and Phenylalanine in an Immunoglobulin Monoclonal Antibody

Shuxia Zhou · Olivier Mozziconacci · Bruce A. Kerwin · Christian Schöneich

Received: 28 August 2012 / Accepted: 15 October 2012 / Published online: 15 February 2013  
© Springer Science+Business Media New York 2013

## ABSTRACT

**Purpose** Metal-catalyzed oxidation (MCO) of proteins is of primary concern in the development of biotherapeutics as it represents a prominent degradation pathway with potential undesired biological and biotherapeutic consequences.

**Methods** We developed a fluorogenic derivatization methodology to study the MCO of IgG1 using a model oxidation system, CuCl<sub>2</sub>/L-ascorbic acid.

**Results** Besides the oxidation of Met, Trp and His residues, we detected significant oxidation of Phe and Tyr in IgG1.

**Conclusion** The fluorogenic derivatization method provides an alternative approach for the rapid detection of oxidized Tyr and Phe as their benzoxazole derivatives by fluorescence spectrometry and size exclusion chromatography coupled to fluorescence detection.

**KEY WORDS** ABS fluorogenic tagging/derivatization · immunoglobulin G (IgG) monoclonal antibody (mAb) · metal catalyzed oxidation (MCO) · protein degradation · reverse phase liquid chromatography with mass spectrometry (RPLC-MS)

## ABBREVIATIONS

3-AT	3-aminotyrosine
ABS	4-(aminomethyl) benzenesulfonic acid
ACN	acetonitrile
DOPA	3,4-dihydroxyphenylalanine
DTT	dithiothreitol

ESI-MS	electrospray ionization – mass spectrometry
FT-ICR MS	fourier transform ion cyclotron resonance mass spectrometry
IAM	iodoacetamide
IgG	immunoglobulin G
mAb	monoclonal antibody
MCO	metal-catalyzed oxidation
SEC	size exclusion chromatography

## INTRODUCTION

Immunoglobulin G (IgG) monoclonal antibodies (mAbs) represent a rapidly growing biotherapeutic class in the biopharmaceutical industry for the treatment and prevention of diseases by recognizing and eliminating pathogenic antigens (1–3). Compared to small-molecule drugs, mAbs are highly specific, reducing potential side effects. On the other side, mAbs exhibit significantly lower stability due to the strong dependence of their physical-chemical properties on conformation. Oxidation represents a prominent degradation pathway of proteins (4–11), potentially changing potency or causing other undesired pharmaceutical consequences.

The detection and identification of oxidized proteins has been an analytical challenge due to their potentially low abundance and structural complexity. With high demands for the development of biotherapeutic products, the need for an efficient and sensitive analytical tool to detect and identify oxidative protein modification(s) is becoming imperative.

Currently, in proteomic research and the biopharmaceutical industry, mass spectrometry (MS) is a dominant tool to characterize protein structural features, including amino acid sequences, disulfide bond linkages, carbohydrate structures and profiles, other post-translational modifications, and in-process and in-storage degradation. Reverse-phase liquid chromatography (RPLC), size exclusion chromatography

S. Zhou · O. Mozziconacci · C. Schöneich (✉)  
Department of Pharmaceutical Chemistry, University of Kansas  
2095 Constant Avenue  
Lawrence, Kansas 66047, USA  
e-mail: schoneic@ku.edu

B. A. Kerwin  
Department of Process and Product Development, Amgen Inc.  
1201 Amgen Court West  
Seattle, Washington 98119, USA

(SEC) and sodium dodecyl sulfate polyacrylamide gel electrophoresis (SDS-PAGE) are generally used to separate proteins prior to MS analysis. Despite the advantages of mass spectrometry, sample separation, purification and digestion, and data analysis and interpretation are very time-consuming and resource-intensive processes. The complexity of these processes and the expertise necessary to utilize mass spectrometry for protein analysis, in general, require a dedicated expert team. In the pharmaceutical industry, RP-HPLC coupled to UV detection has served as a routine analytical method to monitor Met oxidation as an indicator of IgG oxidation. However, this method does not provide a complete picture of oxidation, or may mislead the assessment of protein degradation; for example, in the heavy chain, Met is not the best representative residue to monitor mAb oxidation.

In biotherapeutic product development, manufacturing and during storage, trace amounts of metal ions are inadvertently and inevitably introduced into the product from excipients and contact materials. Even trace amounts of metal ions can be sufficient to induce metal-catalyzed oxidation (MCO) (10). Generally, for the evaluation of a protein's susceptibility towards MCO, a combination of L-ascorbic acid/Cu(II)/O<sub>2</sub> or L-ascorbic acid/Fe(III)/O<sub>2</sub> has been used as a model system to predominately study reaction mechanisms and to identify oxidation-sensitive amino acids (5,10,12–17). Protein primary sequence, structure and the geometry of the metal-binding sites, as well as the particular oxidation mechanisms inherent to various oxidizing species, play important roles in transitional metal-induced oxidative modifications. The predominantly oxidized amino acids are either directly involved in metal-binding or located at or in close vicinity of metal-binding sites (5,10,12,13,15); thus, the reaction sites are not necessarily exposed to the surface. Amino acids sensitive to MCO are mainly Met, His, Trp, Cys, Lys and Arg (5,10,13,14). The chemical modifications generated in an IgG2 mAb were thoroughly studied under different stress conditions (1 mg/mL < [IgG] < 10 mg/mL, in the presence of 5 mM metal, and 4 mM ascorbic acid), including MCO (14), and only oxidative modifications of Met, Trp and His were identified. No oxidative modifications of Tyr and Phe in IgGs are reported to date, even though Tyr oxidation in small proteins and peptides was reported (18–20). Under conditions of MCO, Tyr can be oxidized to different products, such as 3,4-dihydroxyphenylalanine (DOPA), 2-amino-3-(3,4-dioxocyclohexa-1,5-dien-1-yl) propanoic acid (DOCH) (18), and dityrosine (19,20). Tyr and Phe oxidation was also identified in covalent aggregates of insulin induced by MCO (18). Despite the fact that Tyr can be oxidized to different products, Tyr oxidation in IgG and its detection have not received much attention in accelerated stability studies of protein pharmaceuticals.

Specific oxidation products of Tyr and Phe, DOPA and DOCH, can be successfully derivatized with 4-(aminomethyl)-benzenesulfonic acid (ABS), where the resulting benzoxazole

(21) exhibits a characteristic fluorescence with excitation and emission maxima at 360 nm and 490 nm, respectively (18). Thus, fluorescence can serve as a fast and sensitive approach to detect and characterize Tyr and/or Phe oxidation because of the specificity of the resulting benzoxazole derivatives. To date, no study has been reported to utilize this fluorogenic tagging method to monitor and characterize oxidative degradation of IgG mAbs.

Since IgG mAbs represent a major class of biopharmaceutical products, and the exposure of antibodies to redox-active metal ions is inevitable and inadvertent, the screening for oxidative modifications induced by MCO would provide a valuable approach in evaluating antibody instability during biotherapeutic product development. Here, we provide a fluorogenic derivatization methodology to detect oxidized Phe and Tyr in IgG1 to monitor IgG1 oxidation induced by MCO.

## MATERIALS AND METHODS

### Materials

IgG1 mAb stock solution at 37 mg/mL was supplied by Amgen Inc. (Seattle, WA, USA). The purified antibody was stored in formulation buffer at –80°C. Dithiothreitol (DTT), iodoacetamide (IAM), sodium phosphate dibasic (Na<sub>2</sub>HPO<sub>4</sub>), sodium phosphate monobasic (NaH<sub>2</sub>PO<sub>4</sub>), copper dichloride (CuCl<sub>2</sub>), L-ascorbic acid, potassium ferri-cyanide (K<sub>3</sub>Fe(CN)<sub>6</sub>), and sodium chloride (NaCl) were purchased from Sigma Aldrich (St. Louis, MO, USA). FABRICATOR® was purchased from Bulldog Bio, Inc. (Portsmouth, NH, USA), a distributor of Genovis (Lund, Sweden). All analytical and HPLC grade organic solvents were purchased from Sigma (St. Louis, MO, USA) or VWR Scientific (West Chester, PA, USA). SDS-PAGE running buffer (100 mM Tris, 1.92 M Glycine and 0.1% (w/v) SDS at pH 8.3), sample buffer (100 mM Tris, 100 mM Tricine, and 0.1% (w/w) SDS at pH 8.25) and Precision Plus Protein dual color standards were purchased from Bio-Rad (Hercules, CA, USA). Sequencing-grade trypsin and Glu-C were obtained from Promega Corp. (Madison, WI, USA). ABS was synthesized according to a published protocol (21).

### Metal-Catalyzed oxidation (MCO)

The IgG1 stock solution was exchanged into milliQ H<sub>2</sub>O at 2–8°C using an Amicon® ultra-0.5 centrifugal filter device with a 10 kDa filter membrane (Millipore Inc., Bedford, MA, USA). An aliquot of the IgG1 stock solution in water was diluted to 1.5 mg/mL with 20 mM sodium phosphate buffer (pH6.5). IgG1 oxidation was induced by MCO under

air in the presence of Cu(II)/L-ascorbic acid. The concentration of Cu(II) varied from 10  $\mu$ M to 5 mM (14,16). Considering the relevance to biological and biopharmaceutical conditions (12,22–24), most experiments were performed with low concentrations (10  $\mu$ M) of Cu (II) and 1 mM L-ascorbic acid. An aliquot (1.5 mL) of 1.5 mg/mL IgG1 in 20 mM phosphate (pH6.5) was incubated with 10  $\mu$ M CuCl<sub>2</sub> and 1 mM L-ascorbic acid over 6 h in a 2 mL Eppendorf vial at 37°C in a water bath. An aliquot of oxidized IgG1 solution was sampled at 0, 2, 4, and 6 h. The reaction was quenched by the addition of 100  $\mu$ M disodium ethylenediaminetetracetate (EDTA). In this paper, we will use several terms that need to be explicitly defined. First, the term “control” will refer to an IgG1 sample, which was treated identically as the MCO sample, but without the addition of CuCl<sub>2</sub> and L-ascorbic acid. Second, the term “reference standard” will refer to an IgG1 solution which was freshly diluted from the IgG1 stock solution and not subject to any manipulation related to MCO. The control and the reference standard, respectively, were used to evaluate i) the impact, if any, of the in-process manipulation on IgG1 instability and ii) the method to monitor the IgG1 quality. In the discussion, the same definitions were applied to the control and reference standard.

### MCO Monitored by Size Exclusion Chromatography (SEC)

The MCO of IgG1 was monitored by SEC coupled to a diode array detector. The separation of monomer and degradation products, aggregates (high molecular weight species, soluble aggregates) and fragments (low molecular weight species), was achieved by an isocratic elution at 0.7 mL/min over 40 min with a Shimadzu ultra performance liquid chromatography (UPLC) system equipped with TSK-GEL® G3000SWXL and G2000SWXL columns (7.8×300 mm, 5  $\mu$ m) (Tosoh Biosciences, King of Prussia, PA, USA) connected in line. The mobile phase consisted of 200 mM phosphate and 50 mM NaCl at pH 7.0. An aliquot of 20  $\mu$ L of the IgG1 sample was injected onto the column. The IgG1 stock solution was diluted to 1.5 mg/mL with the mobile phase and used as the reference standard to evaluate the system performance. The elution was monitored by a diode array detector, allowing for the recording of UV spectra in the region of 200–800 nm.

### Cleavage, Reduction, and Alkylation of IgG1

An aliquot of the MCO-treated IgG1 was cleaved at the hinge region using FabRICATOR® at a ratio of 1:1 (w/w) (IgG1/FabRICATOR) for 30 mins at 37°C. Then the disulfide bonds were reduced by DTT (4 mM) by incubating the samples for another 30 mins at 37°C. The thiols resulting from the reduction of the disulfide bonds were alkylated

with 10 mM iodoacetamide for 45 mins, in the dark, at room temperature. An aliquot (20  $\mu$ L) was sampled for RPLC/MS analysis. The remaining solution was used for ABS derivatization (see below). The IgG1 reference standard and the control were cleaved, reduced and alkylated according to the same protocol to evaluate the impact, if any, on IgG1 instability in the absence of MCO reagents.

### Analysis of MCO-Induced Degradation by RPLC-Mass Spectrometry (RPLC-MS)

A 20  $\mu$ L aliquot of IgG1 as well as its control and reference standard after cleavage, reduction and alkylation, were purified by an Amicon® ultra-0.5 centrifugal filter device (Millipore Corp., Bedford, MA, USA) with 50 mM NH<sub>4</sub>HCO<sub>3</sub> (pH8.0). The purified samples were analyzed to evaluate IgG1 degradation induced by MCO using RPLC-MS according to our developed procedure (details are presented in “[Optimization of the LC-MS for Direct Analysis of IgG Fragments](#)”). Briefly, an aliquot of 10  $\mu$ L purified sample was injected onto a non-porous column Presto FF-C18 (15 cm×0.5 mm C18, 2  $\mu$ m) (Imtakt Corp., Philadelphia, PA, USA) on an Acquity RPLC chromatography system (Water Corp., Milford, MA, USA). The chromatographic conditions are detailed below in “[Optimization of the LC-MS for Direct Analysis of IgG Fragments](#).” Each chromatographically separated component was analyzed by means of a SYNAPT G2 high definition mass spectrometer (Waters Corp. Milford, MA, USA). The spectra were acquired using a mass range of 900–3000 amu (amu: atomic mass unit). The data were accumulated for 0.7 s per cycle and processed using the software MassLynx (Waters Corp. Milford, MA, USA). To characterize the polypeptides, the mass-to-charge ( $m/z$ ) ratio distributions were analyzed by maximum entropy (MaxEnt) processing. More details regarding the optimization of this LC-MS analysis are given below in “[Optimization of the LC-MS for Direct Analysis of IgG Fragments](#).”

### Optimization of the LC-MS for Direct Analysis of IgG Fragments

A series of proteins were chromatographically separated after injection of 2–10  $\mu$ L of sample onto the non-porous column Presto FF-C18. A protein mixture standard consisting of intact IgG1 (400 ng/ $\mu$ L), LC (300 ng/ $\mu$ L), Fab-HC (200 ng/ $\mu$ L), Fc-HC (200 ng/ $\mu$ L), bovine serum albumin (30 ng/ $\mu$ L), lysozyme (6 ng/ $\mu$ L) was prepared to test the sensitivity and reproducibility of our LC-MS protocol. The chromatographic separation was achieved by a combination of several linear and non-linear gradients of H<sub>2</sub>O (solvent A) and acetonitrile (ACN, solvent B) containing 0.1% (v/v) formic acid. The column was equilibrated with 15% B at a flow rate of

5  $\mu\text{L}/\text{min}$ . Between 0–3 min, and 3–30 min the eluent composition was linearly increased to 25% B and 35% B, respectively, at a constant flow rate of 5  $\mu\text{L}/\text{min}$ . Between 20–35 min and 35–45 min, the eluent composition was modified to reach 65% and 95% B, respectively, through a non-linear gradient (chromatographic curve #3) at a flow rate of 7  $\mu\text{L}/\text{min}$ . Elution at 95% B was held for 2 min. After 47 min, the flow rate was gradually increased to 10  $\mu\text{L}/\text{min}$  and held for 10 min with 95% B for column washing. The column was re-equilibrated with 15% B at 5  $\mu\text{L}/\text{min}$  for 10 min.

The samples were analyzed by means of a SYNAPT G2 mass spectrometer equipped with a high definition hybrid quadrupole/time-of-flight detector (Waters Corp. Milford, MA, USA). Electrospray ionization (ESI) mass spectra of the proteins were acquired by operating the SYNAPT G2 for maximum resolution with all lenses optimized on the  $[\text{M}+2\text{H}]^{2+}$  ion from the  $[\text{Glu}]^1$ -fibrinopeptide B, and Ar was admitted to the collision cell. The capillary voltage was set to 2.9 kV. The cone voltage was set at 45 V and ramped to 85 V. The voltage of the extraction cone was maintained at 6 V. Source and desolvation were set at 40 L/h, and 250 L/h, respectively. The spectra were acquired using a mass range of 900–3000 amu. The data were accumulated for 0.7 s per cycle and processed using the software MassLynx (Waters Corp. Milford, USA). ESI generated a series of multiply charged ions for a single protein. To characterize the proteins present, the mass-to-charge ratio distributions were analyzed by maximum entropy (MaxEnt) processing. MaxEnt disentangled the  $m/z$  distribution of each mass spectrum produced by the mass spectrometer to present the proteins in the mixture as single peaks on a molecular scale (25–27).

### Feasibility and Optimization of Fluorogenic Tagging of Intact and Cleaved IgG1

After MCO, the intact IgG1 as well as the control and reference standard were dialyzed into 100 mM sodium phosphate buffer (pH 9.0) using Amicon® ultra-0.5 centrifugal filter devices (Millipore Corp. Bedford, MA, USA) for ABS fluorogenic tagging. The feasibility and optimization of ABS tagging of oxidized IgG1 were performed by incubating the oxidized IgG1 with ABS derivatization reagents in the dark at room temperature under the following conditions: i) molar ratios of  $\text{K}_3\text{Fe}(\text{CN})_6$ :IgG1 ranged from 5:1 to 30:1; ii) concentrations of ABS were 2 and 10 mM; and iii) the reaction time spanned over 200 min. An aliquot was sampled at time points of 0, 60, 90, 150 and 200 min. The formation of the resulting fluorescent benzoxazole derivatives of oxidized IgG1 was monitored by a steady-state fluorescence spectrometer and SEC coupled to a fluorescence detector. Similar derivatizing conditions were applied to the reference standard and the control to monitor any

potential derivatization not due to MCO. The optimized ABS-derivatization conditions were applied to oxidized IgG1 as well as its control and reference standard after cleavage, reduction and alkylation for SDS-PAGE and in-gel digestion to identify the oxidized amino acids, and the benzoxazole derivatives of the oxidized Tyr and Phe residues.

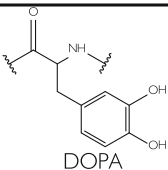
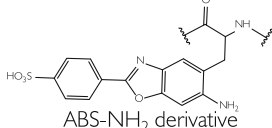
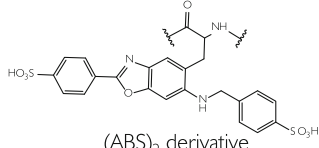
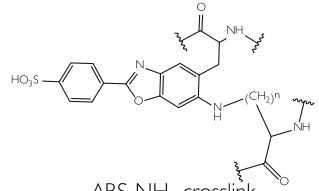
### Steady-State Fluorescence Spectrometry

The benzoxazole fluorescence of the ABS-derivatized IgG1 samples was measured by a Shimadzu RF-5000U fluorescence spectrophotometer (Kyoto, Japan) equipped with a 1-cm quartz cuvette and a 96-well plate model, respectively. The emission and excitation spectra were acquired in a 0.5 mL 1-cm quartz cuvette (Hellma, Plainview, NY, USA), and the fluorescence intensities at  $\lambda_{\text{em}} = 490 \text{ nm}$  ( $\lambda_{\text{ex}} = 360 \text{ nm}$ ) for the ABS derivatized samples as well as the reference standards and controls were measured in a 96-well plate. For both modes, the excitation and emission slit was set at 5 nm.

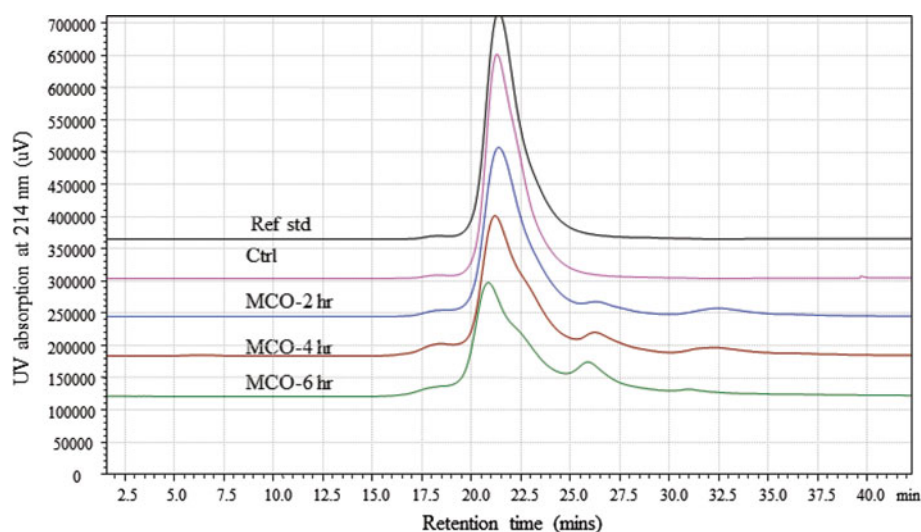
### Sodium Dodecyl Sulfate Polyacrylamide Gel Electrophoresis (SDS-PAGE)

After cleavage, reduction and alkylation, the oxidized IgG1, its control, reference standard and their ABS-

**Table 1** Structure, elementary composition of the modified amino acids and mass shift for the residues which are taken into account for peptide mapping

Structure	Elementary compositions of modifications	Mass shift (Da)
	$\text{O}_1$	+16
	$\text{C}_7\text{H}_4\text{N}_2\text{O}_3\text{S}$	+196
	$\text{C}_{14}\text{H}_{10}\text{N}_2\text{O}_6\text{S}_2$	+366
	$\text{C}_7\text{H}_3\text{O}_3\text{NS}$	+179

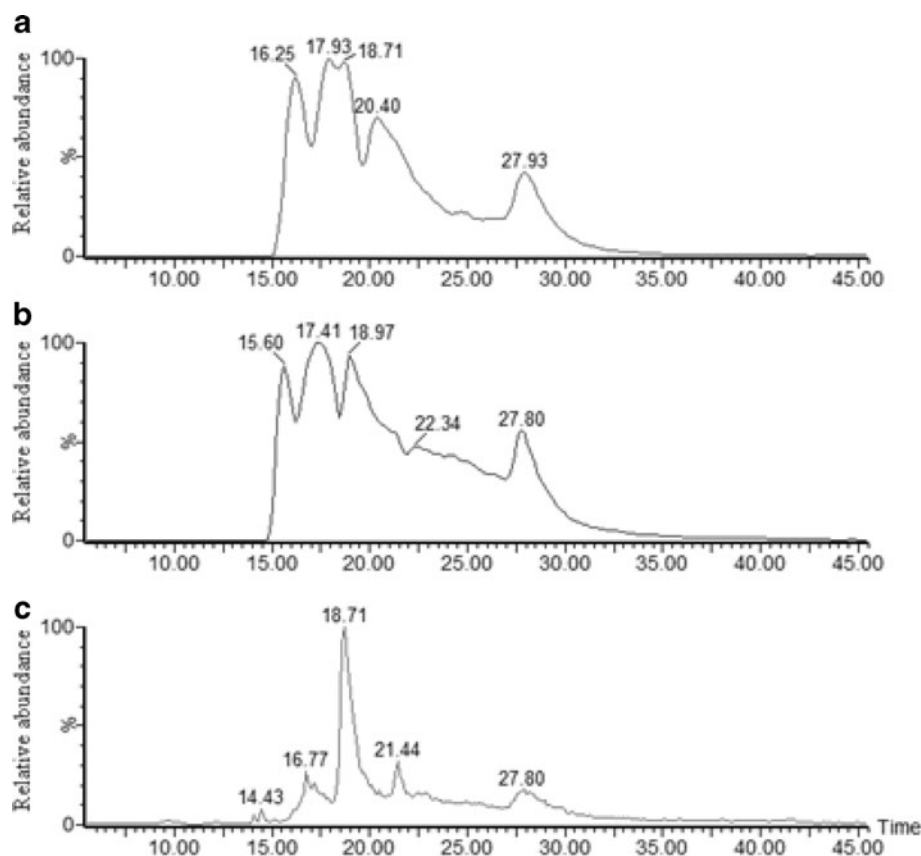
**Fig. 1** SEC-UV chromatograms ( $\lambda = 214$  nm) to monitor IgG degradation induced by metal-catalyzed oxidation (MCO) using the  $\text{CuCl}_2/\text{L}$ -ascorbic acid/ $\text{O}_2$  system.



derivatized samples were independently mixed with SDS-PAGE sample buffer containing 100 mM Tris, 100 mM Tricine, and 0.1% (w/w) SDS at pH 8.25. The samples were boiled at 100°C for 2 mins after mixing. An aliquot of 20  $\mu\text{L}$  of each sample was loaded onto a Novex 4–20% polyacrylamide gel from Invitrogen Inc. (Carlsbad, CA, USA). Molecular Weight Standards, precision plus protein dual color standards from Bio-Rad (Hercules, CA, USA), were also loaded onto the same gel as the

samples. The gel electrophoresis was run under a difference of potential of 250 V for 60 mins using 10-fold diluted running buffer at a temperature maintained at 6°C. Fluorescence visualization of ABS-tagged proteins was recorded by a UV Transilluminator from Fotodyne Inc. (Hartland, WI, USA). Exposing the stained gel to the UVB light source causes the ABS-tagged proteins to fluoresce and become visible. Fluorescent bands of interest were excised for in-gel digestion.

**Fig. 2** RPLC-MS chromatograms of IgG reference standard (a), and the control (b) as well as oxidized IgG (c) after cleavage, reduction and alkylation.





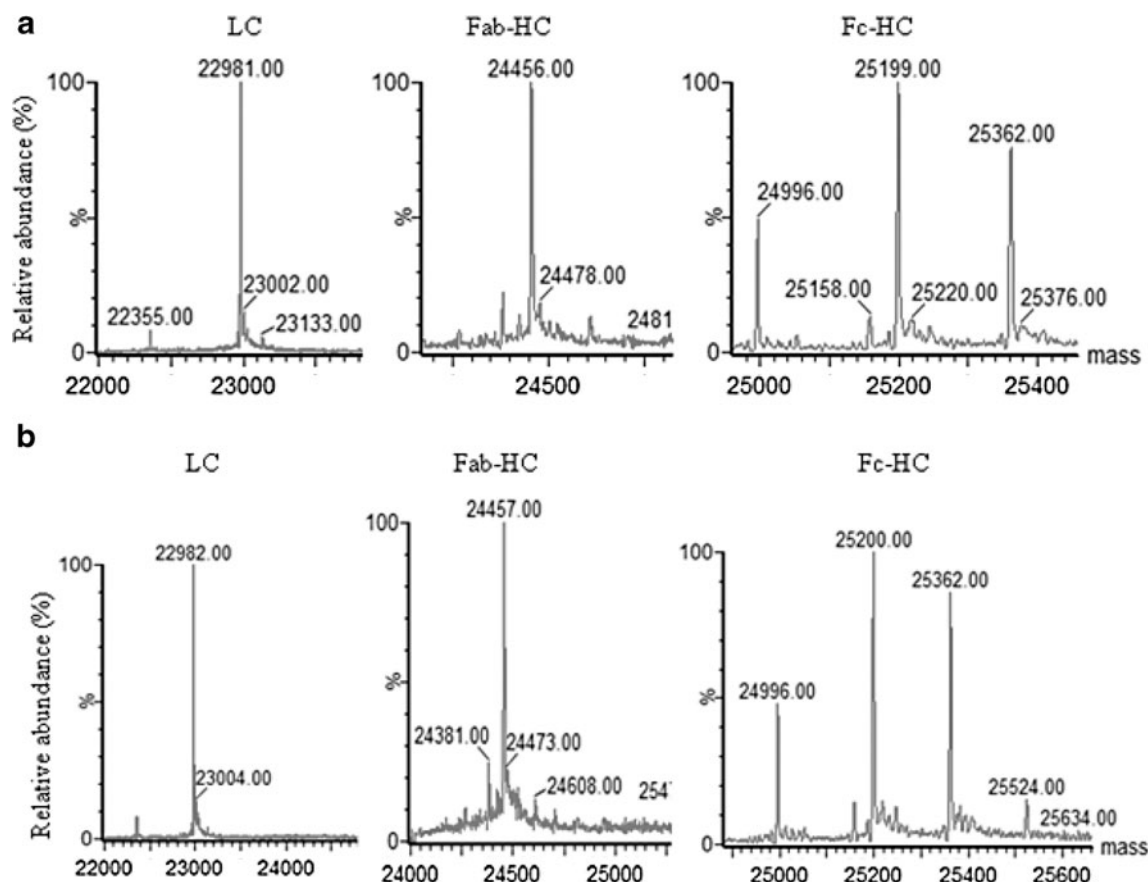


**Fig. 3** Identification of the polypeptides detected by RPLC-MS for IgG1 reference standard (panel a for Fig. 2a) and the control (panel b for Fig. 2b). IgG1 was cleaved at the hinge region and disulfide bonds were reduced and alkylated. The mass of each detected component was obtained by deconvolution of the respective mass-to-charge ( $m/z$ ) ion distribution using MaxEnt.

## In-Gel Digestion

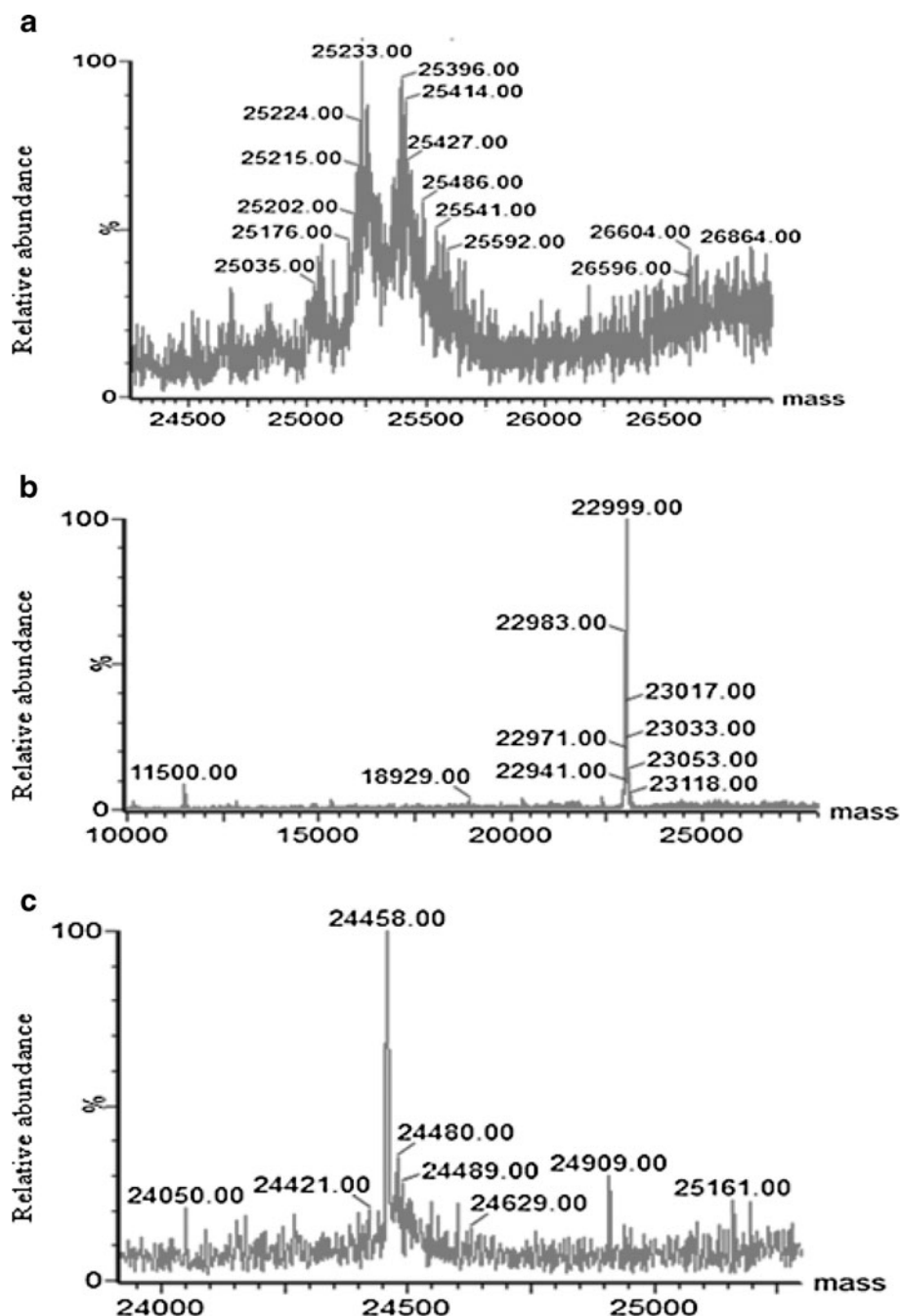
The proteins present in the excised fluorescent bands were digested according to the in-gel digestion protocol described by Shevchenko *et al.* (28). Briefly, the gel slices were first rinsed twice with 100 mM  $\text{NH}_4\text{HCO}_3$  (pH 7.8) in ACN (1:1 v/v) and then rinsed with 100% ACN at room temperature. The gel slices were dried using a SpeedVac from Labconco Corp. (Kansas City, MO, USA). The dried gel slices were incubated for 1 h at 4°C in 125  $\mu\text{L}$  of a Promega® reconstitution buffer for trypsin, containing 5  $\mu\text{g}$  of sequencing-grade trypsin and 2  $\mu\text{g}$  of Glu-C in 1.5-mL Eppendorf vials. An aliquot of 275  $\mu\text{L}$  of 100 mM  $\text{NH}_4\text{HCO}_3$  (pH 7.8) was then added to the samples prior to protein digestion at 37°C overnight. Upon the completion of digestion, the digested protein solutions were transferred into new 1.5-mL Eppendorf vials. The gel slices were rinsed three times with 100% ACN and the rinsing solutions were combined with the digested protein solutions in the new Eppendorf vials. The samples were concentrated using the SpeedVac to reach a final volume of 20  $\mu\text{L}$  for LC-MS/MS analysis.

## CapLC-ESI-LTQ-FT-MS Analysis

The in-gel digested protein samples were subjected to capillary LC-MS/MS experiments using an LTQ-FT mass spectrometer (ThermoFinnigan, Bremen, Germany) under conditions described by Ikehata *et al.* (29). In short, peptides were separated on a reverse-phase *LC Packings PepMap C18* column (0.300  $\times$  150 mm) (Dionex, Sunnyvale, CA, USA) at a flow rate of 10  $\mu\text{L}/\text{min}$  with a linear gradient rising from 0 to 65% ACN in 0.06% aqueous formic acid over a period of 55 mins using a *LC Packing Ultimate Chromatograph* (Dionex, Sunnyvale, CA, USA). LC-MS experiments were performed in a data-dependent acquisition mode using the Xcalibur 2.0 software (Thermo Scientific, Waltham, MA, USA). The five most intense precursor ions in a survey  $\text{MS}^1$  mass spectrum acquired in the FT-ICR over a mass range of 300–2000 amu were selected and fragmented in the linear ion trap by collision-induced dissociation. The ion selection threshold was 500 counts.

The analysis of the MS/MS spectra was performed using MassMatrix (30–32). The theoretical fragments from the parent ions were generated by MassMatrix and then compared to the experimental MS/MS spectra to validate the structures,

**Fig. 4** Identification of the polypeptides detected by RPLC-MS for oxidized IgG1 (panels a, b, and c for Fig. 2c). **(a)** oxidized polypeptides from Fc-HC; **(b)** from LC; **(c)** from Fab-HC. IgG1 was cleaved at the hinge region and disulfide bonds were reduced and alkylated. The mass of each detected component was obtained by deconvolution of the respective mass-to-charge ( $m/z$ ) ion distribution using MaxEnt.



which were taken into account only when the difference between the theoretical and the experimental  $m/z$  of the parent ion was within 0.1 Da. The oxidation of Met (+16 amu), Cys (+16, 32 amu, and 48 amu) and Trp (+4, 16, 20, 32 amu), Phe (+16 and 32 amu), and Tyr (+14 and 16 amu) and the benzoxazole derivatives of oxidized Tyr and Phe (listed in Table I) were built in a customized IgG1 database for identification of the chemical modifications. The elementary compositions of the benzoxazole derivatives of the oxidized Tyr and Phe residues are also listed in Table I.

## RESULTS

### Degradation of IgG1 Induced by MCO

In a 2-mL Eppendorf vial, 1.5 mL of IgG1 at a concentration of 1.5 mg/mL in 20 mM sodium phosphate buffer (pH 6.5) was incubated with 10  $\mu$ M  $\text{CuCl}_2$  and 1 mL ascorbic acid over 6 h at 37°C. IgG1 degradation induced by MCO was monitored at 0, 2, 4, and 6 h by SEC coupled to a diode array detector (Fig. 1). Soluble aggregates ( $t_R = 18.0$  min) were eluted first, followed by monomers ( $t_R = 21.5$  min) and fragments

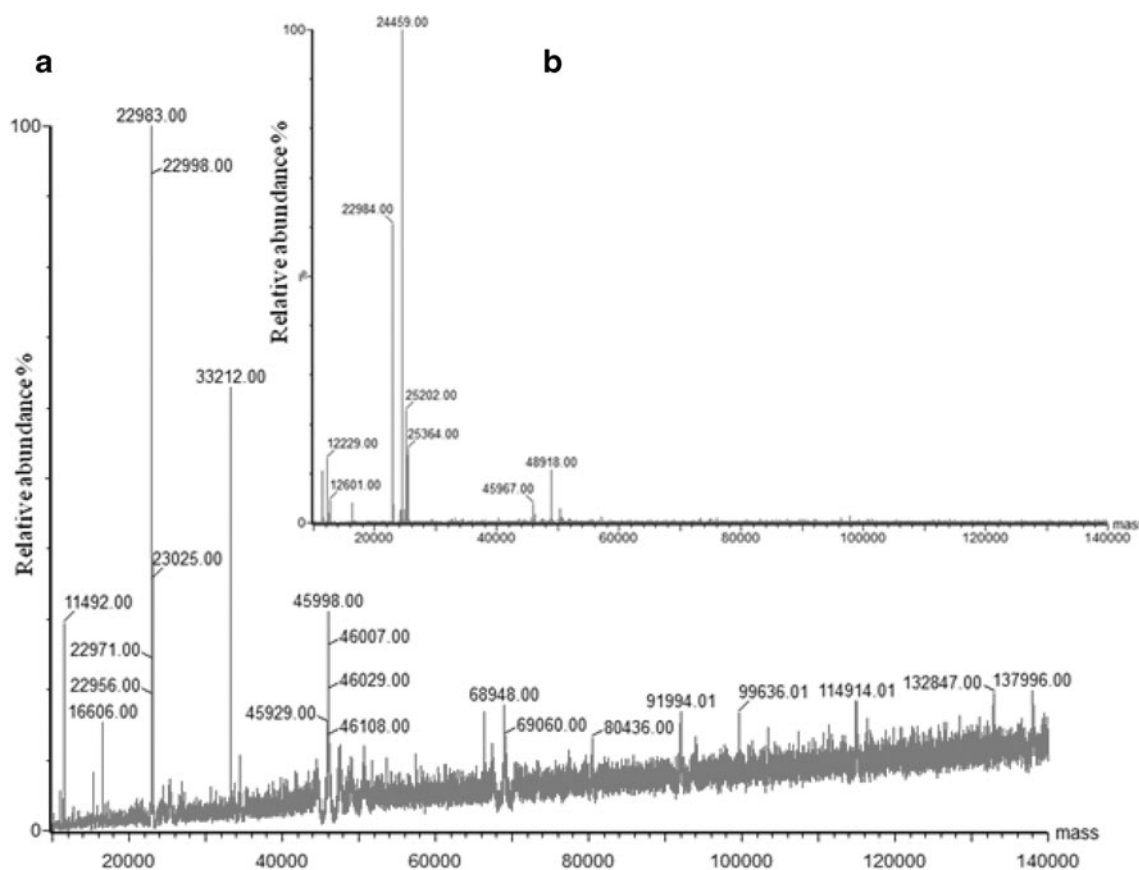


**Fig. 5** Combination of all the MS scans of oxidized IgG1 (**a**) and non-oxidized IgG1 (**b**).

( $t_R$  = 26.0 min) (Fig. 1). The control (Fig. 1, pink) exhibits the same profile as our reference standard (Fig. 1, black). Thus, the processing of IgG1 did not induce additional soluble aggregates and fragments. A prolonged exposure (over 6 h) of IgG1 to MCO reagents ( $\text{CuCl}_2$ /L-ascorbic acid under air) led to the formation of more soluble aggregates and fragments as monitored by UV detection at 214 nm (Fig. 1, blue, dark red and green).

To further characterize the MCO of IgG1, the reference standard, control and oxidized IgG1 were cleaved, reduced and alkylated as described in the section “**Cleavage, Reduction, and Alkylation of IgG1**,” to form Fc-HC, Fab-HC and LC. The resulting polypeptides were analyzed by RPLC-MS. The chromatograms, monitored by MS analysis of the reference standard, control, and oxidized IgG1 are shown in Fig. 2. The chromatograms of the reference standard (Fig. 2a) and the control (Fig. 2b) exhibited the same pattern, which is different from that of the oxidized IgG1 (Fig. 2c). Masses of the polypeptides observed in the control (Fig. 3a) and reference standard (Fig. 3b) confirm that the processing of the IgG1 (in the absence of MCO) did not induce detectable degradation. Indeed, the acquired molecular weights of 22,982 Da for the LC and 24,457 Da for Fab-HC, respectively,

match their expected masses after alkylation. Also, the acquired molecular weights of 24,996 Da, 25,200 Da and 25,362 Da match the expected masses taking into account the glycosylation heterogeneity of the IgG1 Fc-HC (unpublished data). The MCO of IgG1 results in a mass increase of 32 Da (25,201 Da to 25,233 Da and 25,364 Da to 25,396 Da) for the Fc-HC (Fig. 4a). Similarly, new species with mass increases of 16 Da and 34 Da (22,983 Da to 22,999 Da, and 22,983 Da to 23,017 Da) along other products were observed for the IgG1 LC (Fig. 4b). No significant new species were observed for the Fab-HC resulting from MCO (Fig. 4c). The mass spectrometric analysis of the oxidized IgG1 (Fig. 4) indicates that several amino acids may be targeted for oxidative modifications, although the  $\text{MS}^1$  analysis alone cannot detail which amino acid is oxidized. The analysis of oxidized IgG1 as well as its control (Fig. 5) indicate that MCO induced not only oxidative modifications in the IgG1 primary sequence, as described above, but also induced the formation of fragments and/or aggregates, consistent with the data obtained by SEC-UV analysis. For example, a fragment with a mass of 11,492 Da and multiple aggregates with masses of 33,212 Da, 45,998 Da and 68,948 Da etc., were formed due to MCO.



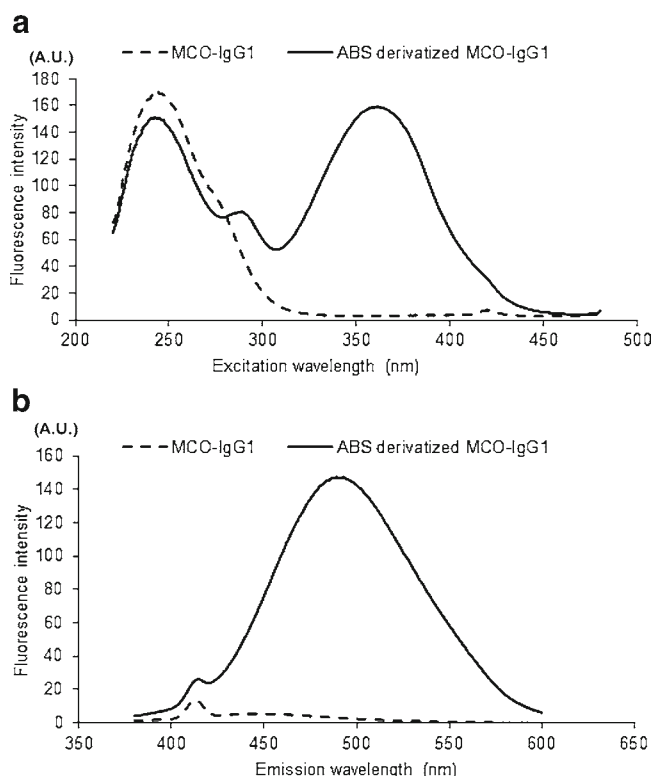


**Fig. 6** Fluorescence spectra for oxidized IgG1 prior to and after ABS derivatization: emission spectra at  $\lambda_{\text{ex}} = 360$  nm (**a**), and excitation spectra at  $\lambda_{\text{em}} = 490$  nm (**b**).

### ABS Derivatization of Oxidized IgG1: Feasibility and Optimization

$\text{CuCl}_2$  and L-ascorbic acid were removed after oxidation of IgG1 by centrifugation through a 10 kDa centrifugal filter (as described in the section “Analysis of MCO-Induced

Degradation by RPLC-Mass Spectrometry (RPLC-MS)”) prior to ABS derivatization. The same procedure was applied to the control. Oxidized IgG1 and its control were incubated with 10 mM ABS and 100  $\mu\text{M}$  of  $\text{K}_3\text{Fe}(\text{CN})_6$  (molar ratio  $\text{K}_3\text{Fe}(\text{CN})_6$  : IgG1 of 10:1) for 1 h in the dark at room temperature. Prior to and post ABS derivatization, the fluorescence emission (370 to 650 nm at  $\lambda_{\text{ex}} = 360$  nm) and excitation (220 to 470 nm at  $\lambda_{\text{em}} = 490$  nm) spectra (Fig. 6) were recorded. For oxidized IgG1 alone, a maximal emission at  $\lambda_{\text{em}} = 410$  nm ( $\lambda_{\text{ex}} = 360$  nm) was observed prior to ABS derivatization (Fig. 6a, dotted line). A maximal emission at  $\lambda_{\text{em}} = 490$  nm with a significantly increased intensity emerged after ABS derivatization (Fig. 6a, solid line). Likewise, at  $\lambda_{\text{em}} = 490$  nm, a maximal excitation at  $\lambda_{\text{ex}} = 360$  nm (Fig. 6b, solid line) was observed after ABS derivatization besides the maximal excitation at  $\lambda_{\text{ex}} = 245$  nm that was present prior to ABS derivatization (Fig. 6b, dotted line). No change in maximal fluorescence emission and excitation wavelengths was observed for the control after and prior to ABS derivatization (data not shown). Additionally, we observed that the fluorescence emission intensity increased at least by 10-fold (Fig. 6a, solid line) after ABS-derivatization in comparison to the non-ABS derivatized oxidized IgG1 (Fig. 6a, dotted line). The increase of fluorescence intensity observed at  $\lambda_{\text{em}} = 490$  nm ( $\lambda_{\text{ex}} = 360$  nm) of the ABS-tagged sample is consistent with the formation of a benzoxazole derivative as presented in Scheme 1 (18). Met, His, and Trp are subject to MCO (5,10,13,14). However, Tyr and Phe are also prone to oxidation. In the presence of  $\text{K}_3\text{Fe}(\text{CN})_6$  and ABS, DOPA and DOCH can be transformed into benzoxazole derivatives via the reactions summarized in Scheme 1. Thus, the characteristic fluorescence ( $\lambda_{\text{em}} = 490$  nm/ $\lambda_{\text{ex}} = 360$  nm) observed after ABS derivatization of the oxidized IgG1 can be rationalized

**Scheme 1** ABS derivatization of oxidized Phe and Tyr to form fluorescent benzoxazole derivatives.

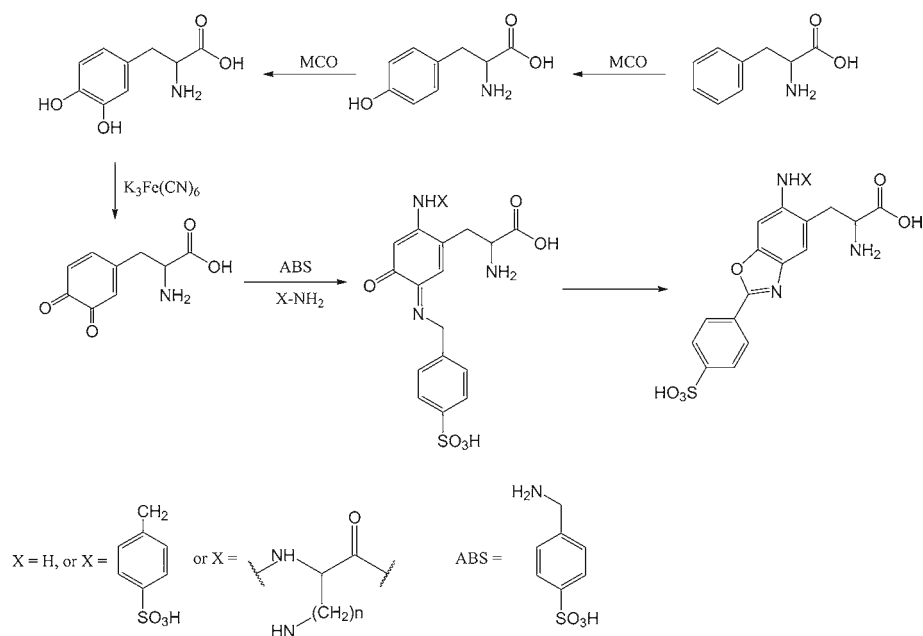
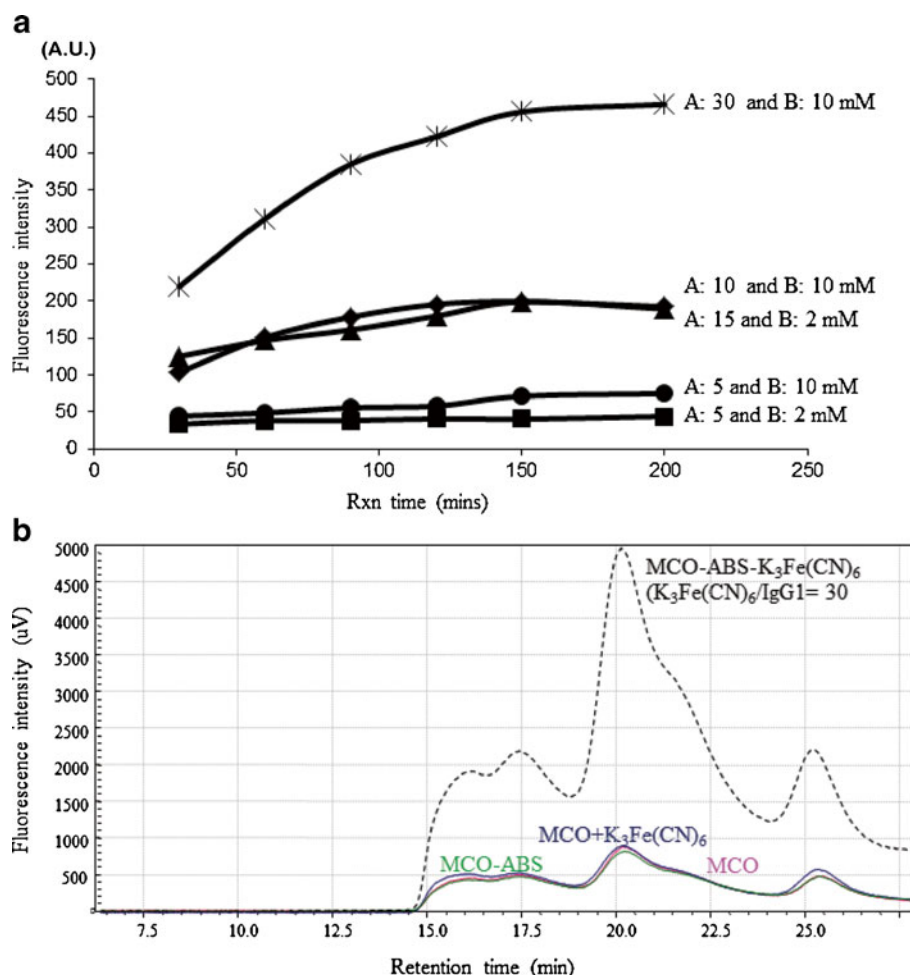


**Fig. 7** (a) Optimization of ABS derivatization of oxidized IgG1 by fluorescence at  $\lambda_{em}=490$  nm ( $\lambda_{ex}=360$  nm) at different molar ratios of  $K_3Fe(CN)_6$ :IgG1 (a) and ABS concentrations (b). (b) SEC-Fluorescence chromatograms ( $\lambda_{em}/\lambda_{ex}=490$  nm/360 nm) of oxidized IgG1 after 200 min of reaction in the presence of ABS.



by the formation of ABS derivatives of DOPA and/or DOCH resulting from the oxidation of Phe and Tyr.

Sharov *et al.* optimized the ABS derivatization conditions for 3-aminotyrosine (3-AT), that is, the optimal molar ratio of  $K_3Fe(CN)_6$  to the peptide was  $\geq 5:1$  in the presence of 2 mM ABS at room temperature for peptide concentrations of 0.1, 1

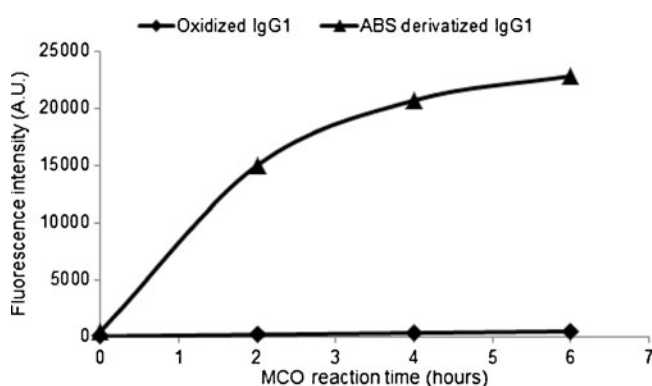
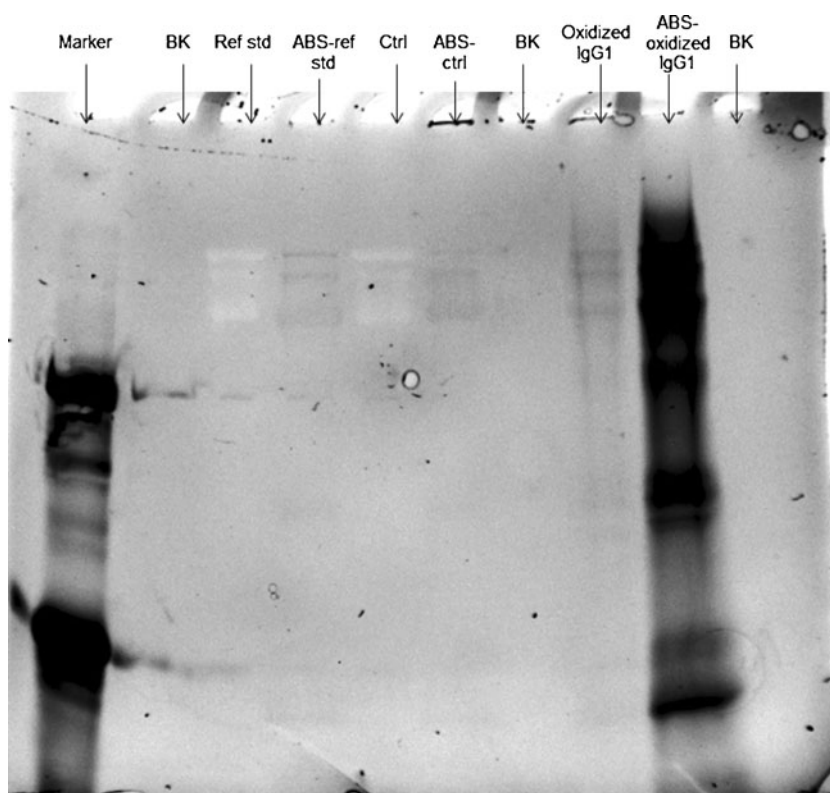


**Fig. 8** Fluorescence ( $\lambda_{em}=490$  nm,  $\lambda_{ex}=360$  nm) of the oxidized products of IgG1 resulting from MCO and followed by ABS derivatization. ABS derivatization conditions were as follows: molar ratio  $K_3Fe(CN)_6$ :IgG1 = 30:1 in the presence of 10 mM ABS. ABS derivatization reaction of the oxidation products was performed at room temperature in the dark.

and 10  $\mu$ M (21). However, this peptide contained only one 3-AT residue for derivatization. Since IgG1 contains twenty seven Tyr and sixteen Phe residues and MS analysis indicated the presence of several oxidized amino acids, it was necessary to optimize the ABS derivatization conditions specifically for the oxidized IgG1. Samples containing the oxidized IgG1 were mixed with different amounts of  $K_3Fe(CN)_6$  and ABS. The molar concentration of IgG1 was maintained at 10  $\mu$ M. The fluorescence intensity of the samples was monitored over 200 min at  $\lambda_{em}=490$  nm ( $\lambda_{ex}=360$  nm) (Fig. 7a). At fixed molar ratios of  $K_3Fe(CN)_6$ :IgG1 = 5:1 and 15:1, the concentrations of ABS at 2 mM and 10 mM did not show significantly different fluorescence, indicating that the ABS concentration was sufficient for derivatization of the oxidized protein. However, an increase of the molar ratio of  $K_3Fe(CN)_6$ :IgG1 resulted in a significant increase of the fluorescence intensity. The latter can be rationalized by the fact that multiple oxidized Tyr and Phe residues are available for ABS derivatization. The derivatization time also affected the fluorescence intensity. A plateau was reached after 150 min. Importantly, the incubation of the oxidized IgG1 with either ABS or  $K_3Fe(CN)_6$  did not produce any additional fluorescence background monitored by fluorescence spectroscopy.

**Fig. 9** SDS-PAGE electropherogram and fluorescence visualization of oxidized IgG1 after ABS derivatization. Fluorescence was recorded by UV Transilluminator (Fotodyne Inc. Hartland, WI, USA).



Thus, the optimized ABS derivatization conditions for oxidized IgG1 are achieved with a molar ratio  $K_3Fe(CN)_6$ :IgG1 = 30:1, and 10 mM ABS. The derivatization reaction was performed at room temperature in the dark for 60–90 min.

To confirm the optimized ABS derivatization conditions, SEC coupled to a fluorescence detector was employed to analyze oxidized IgG1, a mixture of oxidized IgG1 and  $K_3Fe(CN)_6$ , a mixture of oxidized IgG1 and ABS, and ABS-derivatized IgG1 after 90 min storage in the dark at room temperature. The fluorescence (Fig. 7b) was monitored at  $\lambda_{em}$  = 490 nm with  $\lambda_{ex}$  = 360 nm. Consistent with our previous results obtained by fluorescence spectroscopy, the optimized molar ratio

of  $K_3Fe(CN)_6$ :IgG1 = 30:1 resulted in a significant increase of the fluorescence intensity (Fig. 7b, dotted line). Moreover, the incubation of IgG1 with either  $K_3Fe(CN)_6$  or ABS alone under the same conditions did not generate additional fluorescent products (Fig. 7b, solid lines), consistent with the results obtained by fluorescence spectroscopy.

#### ABS Derivatization to Monitor Time-Dependent IgG1 Oxidation

IgG1 was exposed to MCO and an aliquot of the solution was sampled at 0, 2, 4, and 6 h to evaluate the reaction

**Table II** Natures and Positions of the Oxidized Amino Acid Residues

Oxidized residues	Oxidation products	Location	Position	Oxidized/Non-Oxidized
Tyr	3,4-hydroxyphenylalanine (DOPA), quinone	LC	38, 88, 101	3/11
		HC	60, 94, 95, 274, 315, 403	6/16
Phe	hydroxyphenylalanine, DOPA, quinone	LC	103	1/4
		HC	79, 122, 146, 166, 237, 239, 271, 401, 419	9/12
Trp	kynurenine, hydroxyl-Trp, 3-hydroxy kynurenine	LC	37, 191	2/3
		HC	48, 273, 413	3/10
His	2-ox-histidine	HC	54, 220, 281, 306, 431	5/10
Met	methionine sulfoxide, methionine sulfone	HC	248	1/11

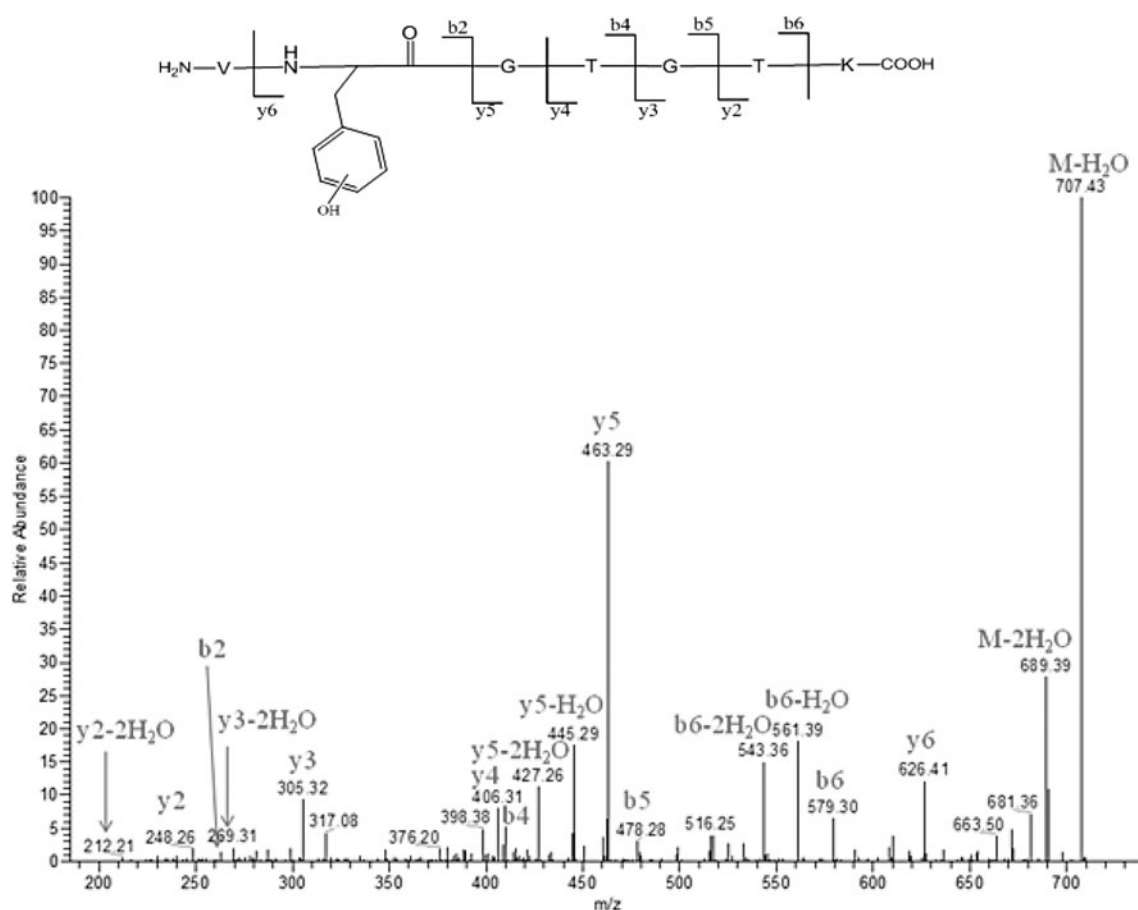


**Fig. 10** Collision-induced dissociation (CID) obtained on an FT-ICR mass spectrometer for the peptide VF(+16 amu)GTGTK [102:108]. The peptide is the result of tryptic digestion of oxidized IgG1 after ABS derivatization.

progress of MCO through ABS derivatization. The control protein was processed in the same way as the oxidized protein. At each time point, the MCO was terminated by the addition of EDTA. Prior to ABS derivatization, the reaction mixtures were dialyzed into sodium phosphate buffer (100 mM, pH 9.0). The progress of MCO was monitored by tagging the IgG1 with ABS using our optimized conditions (see above). The fluorescence intensity at  $\lambda_{em} = 490$  nm ( $\lambda_{ex} = 360$  nm) was measured prior to and after ABS derivatization of the oxidized IgG1 samples and their respective controls. The controls as well as their respective ABS treated controls did not exhibit fluorescence. The fluorescence intensities obtained prior to and after ABS derivatization of the oxidized IgG1 were plotted against the reaction time (Fig. 8). Prior to ABS derivatization, the oxidized IgG1 exhibited very low intrinsic fluorescence. The fact that the fluorescence intensity increased significantly after ABS derivatization of the oxidized IgG1, indicates that the residues of Tyr and/or Phe were oxidized and subsequently derivatized by ABS. Our data show that oxidation of Phe and Tyr occurred within 2 h of MCO.

### SDS-PAGE Visualization of ABS-Derivatized Oxidized IgG1

SDS-PAGE analysis was performed to visualize ABS derivatization of the oxidized IgG1 prior to in-gel digestion. The oxidized IgG1, and the control as well as the reference standard were first cleaved, reduced and alkylated. An aliquot of each sample was incubated with ABS and  $K_3Fe(CN)_6$  at the optimized conditions for ABS derivatization. An aliquot of 5  $\mu$ L of the Molecular Weight Standards was loaded into lane 1 of the SDS-PAGE gel. Lane 2, 7 and 10 were left blank to monitor the background. An aliquot of 20  $\mu$ L of each of the following IgG1 was loaded onto the gel: i) reference standard prior to and after ABS derivatization, ii) control prior to and after ABS derivatization, and iii) oxidized IgG1 prior to and after ABS derivatization. The fluorescence was recorded by a UV Transilluminator (Fotodyne Inc., Hartland, WI, USA) as presented in Fig. 9. Clearly, only ABS derivatization of the oxidized IgG1 (lane 9) exhibited a strong fluorescence. This observation confirms our results obtained by fluorescence spectroscopy and SEC analysis coupled to fluorescence detection. The fluorescent lane 9 in Fig. 9 was excised from the gel

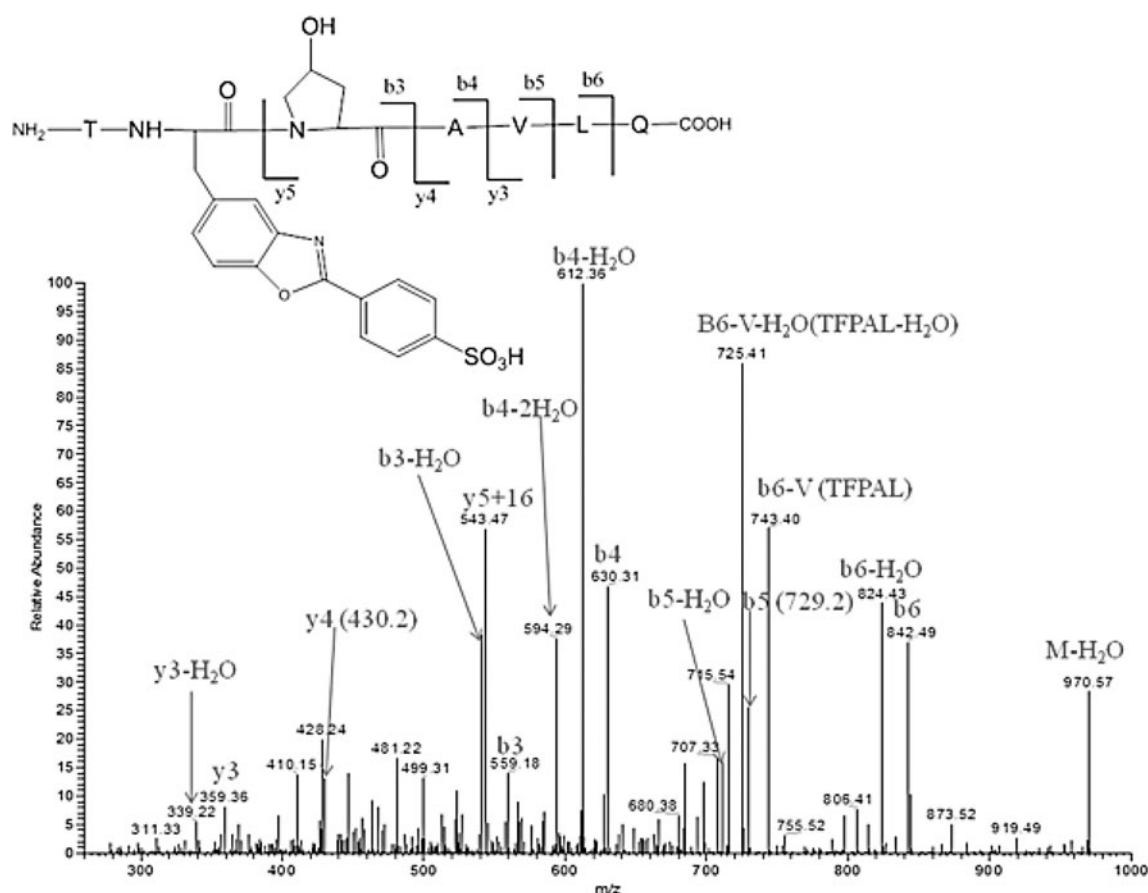


**Fig. 11** Collision-induced dissociation (CID) obtained on an FT-ICR mass spectrometer for the peptide TF(+181 amu)P(+16 amu)AVLQ. The peptide is the result of tryptic digestion of oxidized IgG1 after ABS derivatization.

for in-gel digestion to identify the oxidized amino acids and the benzoxazole derivatives of the oxidized Phe and Tyr residues. The fact that no fluorescence was observed for the ABS-derivatized IgG1 reference standard and the control is consistent with the results obtained by RPLC/MS analysis. That is, the processing of IgG1 did not induce any oxidative modifications. Therefore, we can conclude that any oxidative modifications in the oxidized IgG1 were induced by MCO.

### Identification of ABS Derivatives and Oxidized Amino Acids

The fluorescent lane 9 from the SDS-PAGE (Fig. 9) was excised and subjected to in-gel digestion. The resulting proteolytic peptides were analyzed by means of capillary LC-ESI-LTQ-FT-MS. The purpose of this analysis was to map the oxidative modifications and benzoxazole derivatives in the primary sequence of oxidized IgG1. The oxidized amino acids identified in oxidized IgG1 are summarized in Table II. Besides the oxidation of His, Met and Trp, we report the oxidation of Tyr and Phe residues. In fact, three out of eleven Tyr, two out of three Trp, and one out of four Phe residues located in the IgG1 LC, and six

out of sixteen Tyr, three out of ten Trp, nine out of twelve Phe, five out of ten His and one out of eleven Met residues in the IgG1 HC were oxidized by MCO when IgG1 was incubated with 10  $\mu$ M CuCl<sub>2</sub>/1 mM ascorbic acid at 37°C over 6 h.

Four MS/MS spectra are presented below to illustrate how the oxidative modifications were rationalized from the MS/MS analysis of the proteolytic peptides obtained after digestion of oxidized IgG1. The b and y fragments used in the discussion below for MS/MS analysis refer to the cleavage sites defined by Roepstorff (33).

**Hydroxylation of Phe.** MS/MS data displayed in Fig. 10 indicate that Phe-103 in the IgG1 LC is hydroxylated. The b2 fragment shows a mass increase of 16 Da compared to the b2 fragment of non-oxidized IgG1 indicating that the addition of one oxygen atom is located either to Val or Phe. The series of the fragment ions of b4-b6 and y2-y5 show that none of the amino acids in the sequence GTGTK, C-terminal to Phe is oxidized. The mass increase of 163 Da (147 Da for Phe + 16 Da) from the y5 fragment to y6 confirms that Phe in the tryptic peptide VFGTGTK is oxidized. We cannot determine the position of the hydroxylation from the information obtained here since Phe



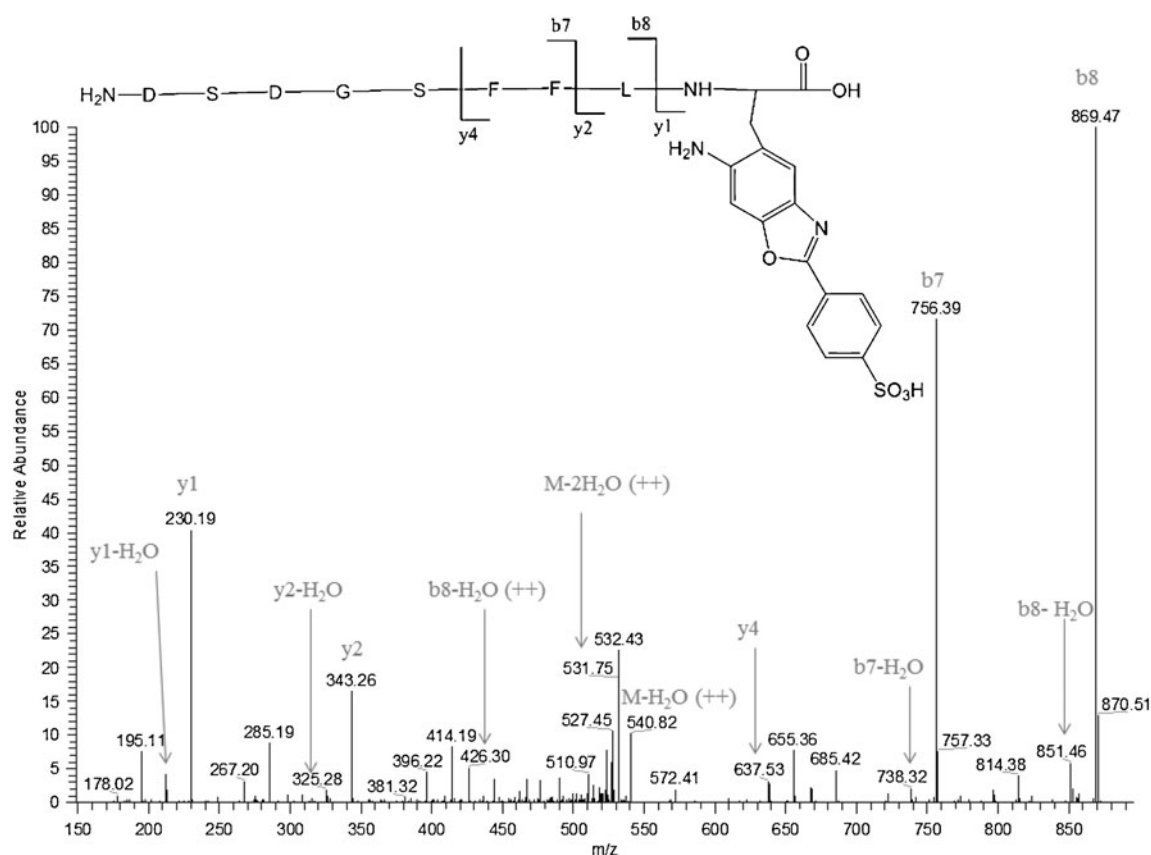


**Fig. 12** Collision-induced dissociation obtained on an FT-ICR mass spectrometer for the peptide, DSDGSFFLY(+196 amu). The peptide is the result of tryptic digestion of oxidized IgG1 after ABS derivatization.

hydroxylation can occur in ortho, meta or para position (34). Only hydroxylation of Phe at the para position leads to the formation of Tyr.

**ABS Derivatization of Oxidized Phe.** The formation of a benzoxazole derivative of oxidized Phe-166 in HC in the sequence of TFPVLQ is indicated by the MS/MS data presented in Fig. 11. The fragment ions y3 and y4 indicate that the sequence of AVLQ is not oxidized and derivatized. The presence of the fragment ion y5+16 Da suggests the formation of a hydroxyl group at Pro in the HC (35). Therefore, the additional mass increase of 181 Da is localized to the sequence TF. The series of b3-b6 fragment ions also confirm a mass increase of 197 Da in the original sequence TFP. The loss of two molecules of H<sub>2</sub>O from the b4 fragment ion is likely due to the presence of two hydroxyl functions within the sequence of the b4 fragment ion. Because the non-oxidized peptide generates a b4 fragment ion with only one Thr, the loss of the second molecule of H<sub>2</sub>O from the b4 fragment ion of the oxidized peptide is therefore likely due to the presence of the hydroxylated Pro. Therefore, we can assign the mass increase of 181 Da to Phe corresponding to the addition of one molecule of ABS. The formation of the benzoxazole group is possibly facilitated by the amide between the original Phe and the Pro residue. The analysis of

the fragment ions is completed by the assignment of the fragment ion TF(+181 amu)P(+16 amu)AL with  $m/z$  of 743.40 and the one with  $m/z$  of 725.41, corresponding to the loss of one molecule of H<sub>2</sub>O from TF(+181 amu)P(+16 amu)AL, respectively. These two fragments are likely formed by a cleavage of Val from b6 and b6-H<sub>2</sub>O, respectively.

**ABS Derivatization of Oxidized Tyr.** ABS derivatization of oxidized Tyr-403 in IgG1 HC is characterized by the MS/MS fragmentation of the parent ion DSDGSFFLY(+196 amu) (Fig. 12). The presence of the y1 and y2 fragment ions indicate a mass increase of 196 Da on the C-terminal Tyr residue. The fragment ion b8 confirms that none of the amino acids in the sequence DSDGSFFL is oxidized. The observation of a mass increase of 196 Da suggests that Tyr was oxidized and subsequently derivatized by ABS. The structure of the benzoxazole derivative is presented in Fig. 12, which contains an amine substituted in the 6-position, consistent with the data of Sharov *et al.* (21).

MS/MS spectra presented in Fig. 13 demonstrate that Tyr-315 in HC is oxidized and subsequently derivatized by ABS. The MS/MS spectrum of the tryptic peptide W(+16 amu)LNGKEY(+179 amu)K shows a mass increase of 179 Da located at Tyr and 16 Da increase located at Trp. Such peptide should have a  $m/z$  of 1232.50. The presence of

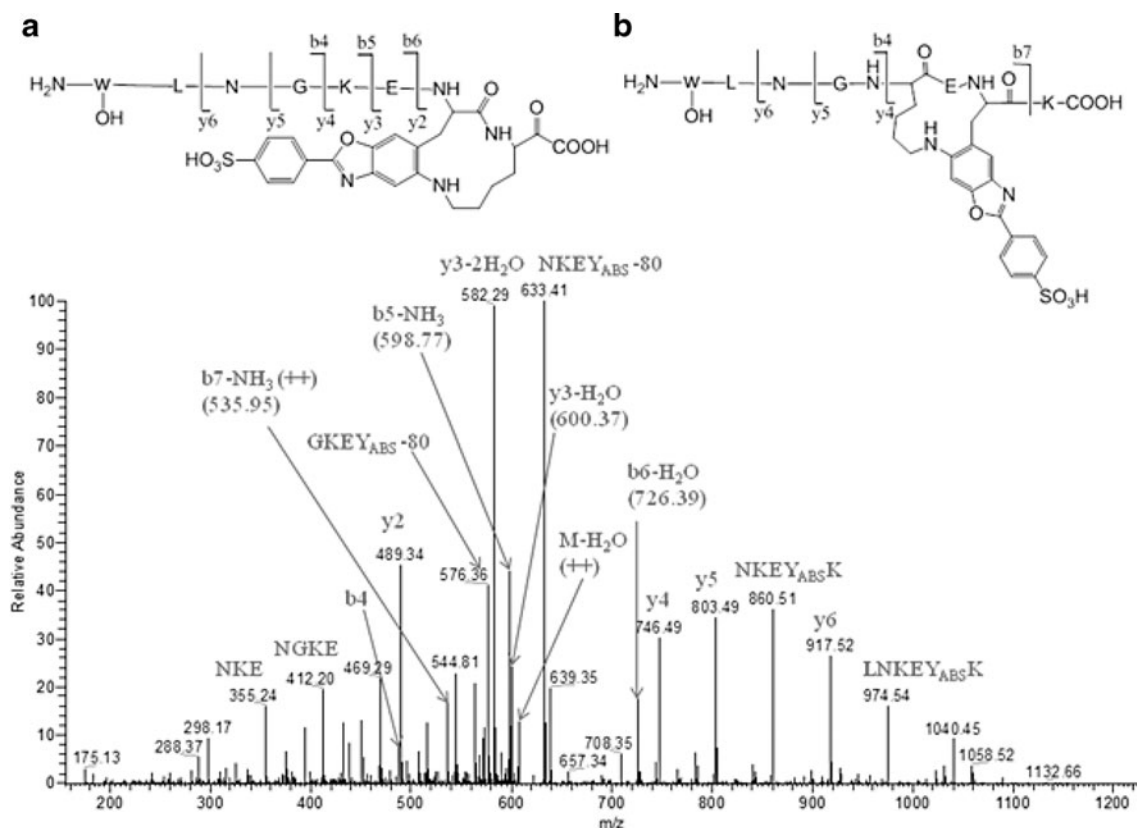


**Fig. 13** Collision-induced dissociation obtained on an FT-ICR mass spectrometer for the peptide W(+16 amu)LNGKEY(+195 amu)K. The peptide is the result of tryptic digestion of oxidized IgG1 after ABS derivatization.

the ion with  $m/z$  of 607.99 (assigned to the  $[M+2H-H_2O]^{2+}$  ion) along with the observation of the series of  $y_2$ - $y_6$  and  $b_4$ - $b_6$  fragment ions suggest that i) the oxidized Tyr is derivatized by ABS, and ii) the formation of a cyclic product involving Lys-316 (Fig. 13a). The structure involving the C-terminal Lys-316 is also supported by the formation of the internal fragment NGKE ( $m/z$  412.20). Meanwhile, the series of  $b_4$ ,  $b_7$  and  $y_4$ - $y_6$  fragment ions, and internal fragment of ABS-derivatized GKEY ( $m/z$  576.36), with a loss of 80 Da ( $SO_3H$ ), suggest that ABS derivatization of the oxidized Tyr can also form a cyclic product with Lys-313 (Fig. 13b). This intra-molecular crosslink is the result of the addition of the primary amine ( $-NH_2$ ) from the side chain of Lys-316 or Lys-313 to the benzoxazole group located on the original Tyr-315. This observed structure of a benzoxazole derivative formed through an intramolecular crosslink of a primary amino group to the 6-position is consistent with data of Sharov *et al.* (21).

MS/MS analysis of the tryptic peptides containing Phe-103 (Fig. 10) in the LC confirms that Phe is oxidized to hydroxyphenylalanine. MS/MS analyses of the tryptic peptides containing Phe-166, HC (Fig. 11), Tyr-403, HC (Fig. 12) and Tyr-315, HC (Fig. 13) confirm that Phe and Tyr residues are oxidized and subsequently derivatized by ABS. Although the formation of 5-hydroxytryptophan (5-

HTP) was observed by mass spectrometry, we did not observe the formation of its fluorescent derivative after ABS tagging.

## DISCUSSION

Oxidative modifications of Trp, His and Met residues induced by MCO are well documented (5,12–14,16,17,36), and specifically His has been identified as a target for MCO (12,13,16,17). Luo *et al.* reported the degradation of IgG2 under different conditions of chemical and physical stresses. The authors demonstrated that the residues Met, Trp, and His were oxidized by MCO (14) (under the following conditions: 1 mg/mL < [IgG] < 10 mg/mL, in the presence of 5 mM metal, and 4 mM ascorbic acid). Consistent with this report, we also observed the oxidation of Met, His and Trp residues during the MCO of IgG1. The MS/MS spectra were not presented here for a more detailed analysis since they are well known oxidation products.

To the best of our knowledge, the oxidation of Tyr and Phe residues in IgG has not been reported. Furthermore, the feasibility of using a fluorogenic tag to detect the oxidized Tyr and Phe in a mAb is also first reported here. We are able to obtain MS/MS confirmation of benzoxazole

derivatives of Tyr-315, HC, Tyr-403, HC and Phe-166, HC, consistent with the observed significant fluorescence increase at  $\lambda_{em}=490$  nm ( $\lambda_{ex}=360$  nm) after ABS-derivatization. The abundance of other ABS-tagged Tyr and Phe residues may be sufficiently high for fluorescence detection, but too low for MS/MS analysis. The mapping of oxidized amino acids in the primary sequence of IgG1 indicates that no modifications are identified in the IgG1 complementarity determining regions (CDRs) for antigen binding.

Noteworthy, the quantification of the monomer by SEC-UV has been a well-accepted practice to evaluate protein stability in the biopharmaceutical industry. However, as revealed by our ABS derivatization procedure, we noticed that the fluorescence signal (due to benzoxazole formation) increased not only for the fragments and soluble aggregates, but also for the monomers monitored by SEC-fluorescence detection (Fig. 7b). These observations suggest that the monomers also incorporate oxidized Tyr and/or Phe that are derivatized with ABS. Therefore, the coupling of our ABS-tagging procedure with SEC-fluorescence analysis provides additional information on protein integrity. That is, a stability study monitored by SEC-UV analysis does not provide sufficient information to assess the stability of IgG1. Here, the application of a variety of techniques such as SEC-UV/fluorescence, SDS-PAGE, RPLC-MS and MS/MS allowed us to develop a practical fluorogenic tagging approach to monitor and characterize oxidized Tyr and Phe amino acids to evaluate IgG1 stability.

This paper presents detailing chemistry to detect the formation of oxidation products deriving from Tyr and Phe residues. We estimated per molecule of immunoglobulin, how many of the Tyr, and Phe residues were oxidized and labeled with ABS. Additional work is underway to quantify the fluorogenic products using spectroscopic techniques.

## CONCLUSIONS

Oxidation represents a prominent protein degradation pathway. In this paper, we applied fluorogenic tagging approach to detect the oxidized Phe and Tyr in IgG. Fluorescence detection alone and/or SEC combined with a fluorescence detector would provide a rapid alternative approach for additional information to evaluate protein stability.

## ACKNOWLEDGMENTS AND DISCLOSURES

This research was supported by Amgen Incorporation. The authors thank Dr. Nadya Galeva from the Mass Spectrometry Laboratory at University of Kansas for performing MS measurements on the FT-ICR instrument.

## REFERENCES

1. Brekke OH, Sandlie I. Therapeutic antibodies for human diseases at the dawn of the twenty-first century. *Nat Rev Drug Discov.* 2003;2:52–62.
2. Bebbington C, Yarranton G. Antibodies for the treatment of bacterial infections: current experience and future prospects. *Curr Opin Biotechnol.* 2008;19:613–9.
3. Schrama D, Reisfeld RA, Becker JC. Antibody targeted drugs as cancer therapeutics. *Nat Rev Drug Discov.* 2006;5:147–59.
4. Bee JS, Nelson SA, Freund E, Carpenter JF, Randolph TW. Precipitation of a monoclonal antibody by soluble tungsten. *J Pharm Sci.* 2009;98:3290–301.
5. Li S, Nguyen TH, Schöneich C, Borchardt RT. Aggregation and precipitation of human Relaxin induced by metal-catalyzed oxidation. *Biochemistry.* 1995;34:5762–72.
6. Li S, Schöneich C, Wilson GS, Borchardt RT. Chemical pathways of peptide degradation. V. ascorbic acid promotes rather than inhibits the oxidation of methionine to methionine sulfoxide in small model peptides. *Pharm Res.* 1993;10:1572–9.
7. Stadtman ER. Metal Ion-catalyzed oxidation of proteins: biochemical mechanism and biological consequences. *Free Radic Biol Med.* 1990;9:315–25.
8. Stadtman ER. Oxidation of free amino acids and amino acid residues in proteins by radiolysis and by metal-catalyzed reactions. *Annu Rev Biochem.* 1993;62:797–821.
9. Uversky VN, Li J, Fink AL. Metal-triggered structural transformations, aggregation, and fibrillation of human alpha-synuclein. A possible molecular link between parkinson's disease and heavy metal exposure. *J Biol Chem.* 2001;276:44284–96.
10. Zhao F, Ghezzi-Schöneich E, Aced GI, Hong J, Milby T, Schöneich C. Metal-catalyzed oxidation of histidine in human growth hormone. mechanism, isotope effects, and inhibition by a mild denaturing alcohol. *J Biol Chem.* 1997;272:9019–29.
11. Zhou S, Zhang B, Sturm E, Teagarden DL, Schöneich C, Kolhe P, *et al.* Comparative evaluation of disodium edetate and diethylenetriaminepentaacetic acid as iron chelators to prevent metal-catalyzed destabilization of a therapeutic monoclonal antibody. *J Pharm Sci.* 2010;99:4239–50.
12. Schöneich C. Selective Cu2+/ascorbate-Dependent Oxidation of Alzheimer's Disease Beta-Amyloid Peptides. *Ann N Y Acad Sci.* 2004;1012:164–70.
13. Schöneich C. Mechanisms of metal-catalyzed oxidation of histidine to 2-oxo-Histidine in peptides and proteins. *J Pharm Biomed Anal.* 2000;21:1093–7.
14. Luo Q, Joubert MK, Stevenson R, Ketchum RR, Narhi LO, Wypych J. Chemical modifications in therapeutic protein aggregates generated under different stress conditions. *J Biol Chem.* 2011;286:25134–44.
15. Limand J, Vachet RW. Development of a methodology based on metal-catalyzed oxidation reactions and mass spectrometry to determine the metal binding sites in copper metalloproteins. *Anal Chem.* 2003;75:1164–72.
16. Schöneich C, Williams TD. Cu(II)-Catalyzed Oxidation of Beta-Amyloid Peptide Targets His13 and His14 over His6: Detection of 2-Oxo-Histidine by HPLC-MS/MS. *Chem Res Toxicol.* 2002;15:717–22.
17. Schöneich C, Williams TD. Cu(II)-Catalyzed Oxidation of Alzheimer's Disease Beta-Amyloid Peptide and Related Sequences: remarkably different selectivities of neurotoxic  $\beta$ AP1-40 and Non-Toxic  $\beta$ AP40-1. *Cell Mol Biol.* 2003;49:753–61.
18. Torosantucci R, Mozziconacci O, Sharov V, Schöneich C, Jiskoot W. Chemical Modifications in Aggregates of Recombinant Human Insulin Induced by Metal-Catalyzed Oxidation: covalent cross-linking via michael addition to tyrosine oxidation products. *Pharm Res.* 2012;29:2276–93.

19. Dubinina EE, Gavrovskaya SV, Kuzmich EV, Leonova NV, Morozova MG, Kovrugina SV, *et al.* Oxidative modification of proteins: oxidation of tryptophan and production of dityrosine in purified proteins using Fenton's system. *Biochemistry*. 2002;67:343–50.
20. Huggins TG, Wells-Knecht MC, Detorie NA, Baynes JW, Thorpe SR. Formation of o-Tyrosine and Dityrosine in Proteins During Radiolytic and Metal-Catalyzed Oxidation. *J Biol Chem*. 1993;268:12341–7.
21. Sharov VS, Dremina ES, Galeva NA, Gerstenecker GS, Li X, Dobrowsky RT, *et al.* Fluorogenic Tagging of Peptide and Protein 3-Nitrotyrosine with 4-(Aminomethyl)-benzenesulfonic Acid for Quantitative Analysis of Protein Tyrosine Nitration. *Chromatographia*. 2010;71:37–53.
22. Zhou S, Evans B, Schöneich C, Singh SK. Biotherapeutic Formulation Factors Affecting Metal Leachables from Stainless Steel Studied by Design of Experiments. *AAPS PharmSciTech*. 2012;13:284–94.
23. Zhou S, Schöneich C, Singh SK. Biologics Formulation Factors Affecting Metal Leachables from Stainless Steel. *AAPS PharmSciTech*. 2011;12:411–21.
24. Zhou S, Singh S, Lewis L. Metal Leachables in Therapeutic Biologic Products: Origin, Impact and Detection. *Am Pharm Rev*. 2010;13:76–80.
25. Ferrige AG, Seddon MJ, Green BN, Jarvis SA, Skilling J. Disentangling Electrospray Spectra with Maximum-Entropy. *Rapid Commun Mass Spec*. 1992;6:707–11.
26. Ferrige AG, Seddon MJ, Jarvis S. Maximum-Entropy Deconvolution in Electrospray Mass-Spectrometry. *Rapid Commun Mass Spec*. 1991;5:374–7.
27. Ferrige AG, Seddon MJ, Skilling J, Ordsmith N. The Application of Maxent to High-Resolution Mass-Spectrometry. *Rapid Commun Mass Spec*. 1992;6:765–70.
28. Shevchenko A, Wilm M, Vorm O, Mann M. Mass Spectrometric Sequencing of Proteins from Silver-Stained Polyacrylamide Gels. *Anal Chem*. 1996;68:850–8.
29. Ikehata K, Duzhak TG, Galeva NA, Ji T, Koen YM, Hanzlik RP. Protein Targets of Reactive Metabolites of Thiobenzamide in Rat Liver *in Vivo*. *Chem Res Toxicol*. 2008;21:1432–42.
30. Xu H, Freitas MA. A Mass Accuracy Sensitive Probability Based Scoring Algorithm for Database Searching of Tandem Mass Spectrometry Data. *BMC Bioinforma*. 2007;8:133.
31. Xu H, Freitas MA. MassMatrix: a Database Search Program for Rapid Characterization of Proteins and Peptides from Tandem Mass Spectrometry Data. *Proteomics*. 2009;9:1548–55.
32. Xu H, Yang L, Freitas MA. A Robust Linear Regression Based Algorithm for Automated Evaluation of Peptide Identifications from Shotgun Proteomics by Use of Reversed-Phase Liquid Chromatography Retention Time. *BMC Bioinforma*. 2008;9:347.
33. Roepstorff P, Fohlman J. Proposal for a common nomenclature for sequence ions in mass spectra of peptides. *Biomed Mass Spectrom*. 1984;11:601.
34. Kaur H, Fagerheim I, Grootveld M, Puppo A, Halliwell B. Aromatic Hydroxylation of Phenylalanine as an Assay for Hydroxyl Radicals: Application to Activated Human Neutrophils and to the Heme Protein Leghemoglobin. *Anal Biochem*. 1988;172:360–7.
35. Shacter E. Quantification and Significance of Protein Oxidation in Biological Samples. *Drug Metab Rev*. 2000;32:307–26.
36. Schöneich C, Sharov VS. Mass Spectrometry of Protein Modifications by Reactive Oxygen and Nitrogen Species. *Free Radic Biol Med*. 2006;41:1507–20.